Cleaner Engineering and Technology 20 (2024) 100751

Contents lists available at ScienceDirect

Cleaner Engineering and Technology

journal homepage: www.sciencedirect.com/journal/cleaner-engineering-and-technology

Evaluating sugarcane bagasse fly ash as a sustainable cement replacement for enhanced performance

Ketlynn Passos Alvarenga, Guilherme Chagas Cordeiro *

Laboratory of Civil Engineering, Universidade Estadual do Norte Fluminense Darcy Ribeiro, Campos dos Goytacazes, RJ, 28013-602, Brazil

ARTICLE INFO

Keywords:
Sugarcane bagasse fly ash
Pozzolan
Pozzolanic activity
Grinding
Durability

ABSTRACT

This study evaluated the potential of sugarcane bagasse fly ash, collected from boiler exhaust stacks via a bypass pipe, as a renewable supplementary cementitious material. The bagasse fly ash was ground into three different particle sizes (D_{50} of 10, 20, and 30 μm) and characterized in terms of morphology, porosity, specific surface area, and pozzolanic activity. The influence of the ashes on paste hydration was investigated using isothermal calorimetry. Mortars were then tested with 20% cement replacement by fly ash, analyzing packing density, compressive strength evolution, and durability against sulfuric acid. Results indicated the suitability of the fly ash as a supplementary cementitious material, with low contamination and greater pozzolanic activity at smaller particle sizes. This enhanced initial hydration and long-term strength, with finer ashes showing superior mechanical properties when compared to the reference mortar (an 8% increase). Mortars with fly ash exhibited higher packing density and reduced mass loss under sulfuric acid attack, but increased water absorption and capillarity, alongside decreased compressive strength compared to the reference. Briefly, the findings highlighted that the potential of bagasse fly ash as a promising low cost and eco-beneficial material for sustainable construction practices.

1. Introduction

It is imperative to act now to reduce global environmental impacts by combating CO_2 emissions and preserving our planet for future generations. The cement industry plays a pivotal role in the necessary reduction of global emissions, requiring innovation and more sustainable practices to build a greener and healthier future for our planet. On the other hand, industrial waste discharged into the soil poses a significant environmental threat and can lead to soil contamination, compromising agricultural land quality, groundwater, and overall ecosystem health (Mohan et al., 2023). Sales and Lima (2010) emphasized the negative impact of improper disposal and the use of these residues as fertilizers, especially in powder form, due to their low soil enrichment potential.

In this scenario, sugarcane bagasse ash (SCBA), an abundant residue generated globally every year, is of paramount importance, particularly in the cement industry, with its silica-rich composition making it an attractive and valuable resource. Thus, SCBA is a promising pozzolanic material, recognized in several studies conducted in recent decades (Ahmad et al., 2021; Minnu et al., 2021). It is mainly generated via the conventional methods used in the sugar and ethanol agroindustry, which involve storing sugarcane bagasse outdoors for subsequent calcination in boilers.

Bagasse is used to produce electricity, primarily via direct combustion, whereby chemical energy is converted into heat. The ashes resulting from bagasse combustion can be classified as bottom ash, which settles at the bottom of the boiler, or fly ash, which is carried by the gases generated during burning. Bottom ash, generally known as SCBA, has been widely studied in the last two decades, with different production and characterization processes confirming its potential as supplementary cementitious material. Research has demonstrated the positive effects of SCBA on the hydration (Cordeiro and Kurtis, 2017), mechanical properties (Nassar et al., 2022) and durability (Arif et al., 2016) of cementitious systems. Despite its proven benefits and renewability, the large-scale application of SCBA as a pozzolan remains limited, largely due to its variable chemical composition (Mali and Nanthagopalan, 2021a) and the presence of contaminants (Almeida and Cordeiro, 2023) such as quartz and carbonaceous compounds.

Different pretreatment methods have been used to increase SCBA reactivity, the most common being mechanical grinding. This technique increases the specific surface area of material (Cordeiro and Kurtis,

* Corresponding author.
E-mail address: gcc@uenf.br (G.C. Cordeiro).

https://doi.org/10.1016/j.clet.2024.100751
Received 15 February 2024; Received in revised form 14 April 2024; Accepted 3 May 2024
Available online 4 May 2024

2017) and can reduce quartz contamination (Cordeiro et al., 2016). Recalcination has also been adopted to enable SCBA to be used without compromising the hydration reactions of Portland cement (Andreão et al., 2020). Although SCBA is the main focus of research, the new possibility of collecting material from boilers has recently attracted attention from researchers. In this case, bagasse fly ash is separated from flue gases via baghouse dust filters, soot traps, or special collection systems with bypass pipes (Bahurudeen et al., 2014). Due to their collection characteristics, fly ash exhibits less variability in chemical composition and particle size distribution than bottom ash, representing a significant advantage. Indeed, Barbosa and Cordeiro (2021) found that bagasse fly ash produced in a laboratory by density separation of quartz (Andreão et al., 2020) followed by controlled calcination and grinding showed similar behavior to that of a highly reactive rice husk ash. A limitation for the widespread application of this type of sugarcane ash is the absence of selective collection at the mills. However, this is expected to change. Although many sugarcane mills currently rely on outdated boiler technology, trends indicate imminent modernization.

In this context, the present study aimed to assess the potential of bagasse fly ash collected directly from the exhaust stacks of a boiler. The ash was ground into three different particle sizes and then characterized. Additionally, the effect of these ashes on cement paste hydration was investigated by isothermal calorimetry. Mortars were also tested to systematically assess the effect of partially replacing cement (20% in mass) with the bagasse fly ash on packing density, compressive strength over time and durability under sulfuric acid attack.

2. Materials and methods

2.1. Original sugarcane bagasse fly ash (SBFA) and paste-mortar materials

The sugarcane bagasse fly ash used here was collected from a sugarcane ethanol production plant in the city of Campos dos Goytacazes, in Rio de Janeiro state, Brazil. Particulate matter was removed by installing a bypass pipe in the flue gas outlet of a watertube boiler with a pinhole grate. It is important to properly control and remove fly ash from flue gas emissions to prevent atmospheric pollution and comply with environmental regulations (de Almeida et al., 2023).

Class G cement (ABNT NBR 9831, 2020), limestone-blended Portland cement (ABNT NBR 16697, 2018), quartz river sand (fineness modulus of 2.25 and density of 2.66 g/cm^3), standard quartz sand (ABNT NBR 7214, 2015), polycarboxylate-based superplasticizer (1.18 g/cm^3 density and 28.9% oven-dried residue), and deionized water were used to produce the cement pastes and mortars. Ultrafine anatase powder (99.5% purity) was used in Rietveld quantification and calcium hydroxide, calcium carbonate, calcium oxide, aqueous potassium hydroxide, and potassium sulfate were used in pozzolanic activity tests. The acid solution used to attack the mortars was prepared with sulfuric acid. All chemicals were analytical grade and provided by Vetec, Brazil.

2.2. Production and characterization of sugarcane bagasse fly ash samples

After collection, the SBFA sample was homogenized in a Solab SL-34 ball mill with a 10 L alumina jar and 10 kg of spherical aluminum balls (equal number of 22, 13, and 6 mm-wide balls). Open-circuit dry grinding was performed with 1.35 kg of feed material at 28 rpm for 12 min, the minimum time required for the ashes collected at different times to reach similar particle sizes. The ash obtained after homogenization was denominated SBFA30 because its D_{50} value was approximately 30 μm. SBFA30 was used to produce two additional ash samples, with D_{50} of around 20 (SBFA20) and 10 μm (SBFA10) with total grinding times of 45 and 240 min, respectively. The remaining grinding conditions were the same as those adopted for homogenization. Fig. 1 summarizes the methodological procedures used in the production and characterization of the three SBFA samples, as well as the application of these materials in cement-based pastes and mortars.

The chemical composition of the bagasse fly ashes was determined by X-ray fluorescence spectrometry in a Shimadzu EDX-720 analyzer. Loss on ignition (LOI) and density were obtained in accordance with Brazilian technical standards ABNT NM 18 (2012) and ABNT NBR 16605 (2017), respectively. Particle size distribution was assessed in a Malvern Mastersizer 3000 device with a Hydro LV accessory, using deionized water (for SBFA) or pure ethanol (for cement) as dispersant, dispersion with a controlled stirrer at 1200 rpm for 5 min, 1 min of ultrasound, and 16% obscuration. The BET specific surface area and ash porosity were determined from nitrogen gas (N_2) adsorption-desorption

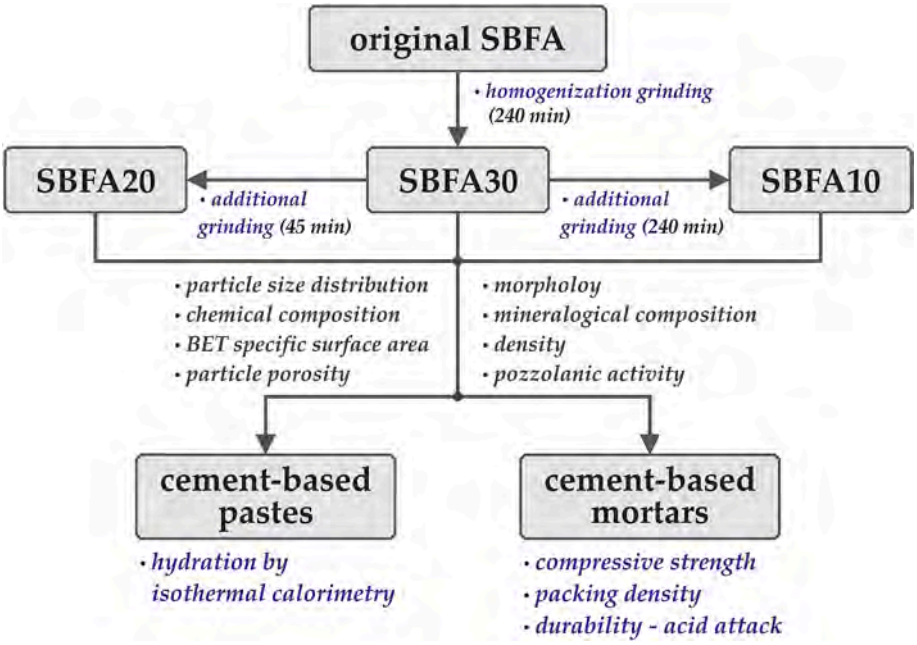

Fig. 1. Flowchart outlining the methodological procedures employed in the study.

analysis using an ASAP 2020 analyzer (Micromeritics). Before testing, the samples were treated at 200 °C for 8 h.

For morphology assessment, the samples were coated with palladium and analyzed under a Zeiss EVO 40 scanning electron microscope. Sample mineralogy was obtained in a Rigaku Miniflex 600 diffractometer using Cu-kα radiation, with tube voltage of 40 kV, 15 mA current, 2θ detector angle between 8 and 70°, angular speed of 5°/min, angular step of 0.03°, and sample spinner. Phases were quantified by the Rietveld method (Liu and Kuo, 1996), using anatase (20% by mass) as an external standard to determine the amorphous content.

Pozzolanic activity was investigated in mechanical performance index, reactivity with lime, and the modified Chapelle tests. To calculate the performance index according to Brazilian standard ABNT NBR 5752 (2014), a control mortar was prepared based on water-to-cement and standard sand-to-cement ratios of 0.48 and 3.0, respectively. Additional mortars were produced by replacing 25% of cement with each of the ashes. Flow-table spreading (ASTM C1437-20, 2020) was fixed at 250 ± 10 mm with specific superplasticizer contents (between 0.05 and 0.19%). The performance indices were calculated by the ratio between the strength of the mortar mixes and control after 28 days of curing in a lime-saturated solution. The 50-mm cubic test specimens were ruptured in a Shimadzu UH-F500kNI universal testing machine at 0.5 mm/min.

The reactivity of the ashes with lime was obtained based on the recommendations of Kasaniya et al. (2019). The mortars consisted of calcium hydroxide, calcium carbonate, and an alkaline solution (281.7 g of deionized water, 1.12 g of potassium hydroxide and 5.60 g of potassium sulfate). The solution-to-SBFA, SBFA-to-calcium hydroxide, calcium carbonate-to-SBFA, and sand-to-binder mass ratios were 0.67, 1.50, 0.12 and 2.50, respectively, considering the binder as the sum of SBFA, calcium hydroxide, and calcium carbonate. Flow-table spreading (ASTM C1437-20, 2020) was fixed at 250 ± 10 mm. Three cubic test specimens (50 mm edge) were prepared for each mix and molded for 24 h. After this period, the molds were wrapped in plastic film and placed in an oven at 50 °C for 48 h, then in a water bath at 40 °C up to 7 days. After curing, the specimens were ruptured under axial compression. The Chapelle test consisted of quantifying fixed hydroxide after mixing 1 g of the sample with 2 g of CaO and 250 g of water, followed by a water bath at 90 °C for 16 h, in line with the recommendations of ABNT NBR 15895 (2010).

2.3. Production and characterization of cement-based pastes

Four pastes were produced for the hydration study, one as reference (P-REF) and three containing the different ashes as partial replacement for 20% cement (P-SBFA10, P-SBFA20, and P-SBFA30). All the pastes had a water-to-binder ratio of 0.4 and superplasticizer content of 0.02 wt %. The pastes were manually stirred with a spatula for 30 s, followed by an electric hand mixer for 30 s at low speed (260 rpm) and then at high speed (600 rpm) for another minute.

Isothermal calorimetry tests were performed in duplicate (about 50 g of each paste) in a Calmetrix I-CAL 2000 isothermal calorimeter at 25 ± 0.1 °C until 72 h of hydration. Approximately 5 min passed between the onset of mixing, placing the container with the paste in the calorimeter, and beginning data registration. Because the pastes were mixed outside the calorimeter, the first hydration peak (caused by adding water to the cement) was not evaluated, and the equipment only accurately detected data from the end of the first reaction peak.

2.4. Mortar production and characterization - compressive strength and acid attack

Four mortars were prepared to assess compressive strength over time and durability under acid attack, one as reference (M-REF) and three with 20% of cement replaced by the SBFA samples (M-SBFA10, M-SBFA20, and M-SBFA30). The water-to-binder and sand-to-binder ratios were 0.48 and 3.0, respectively. Specific superplasticizer contents were used to maintain mortar consistency (ASTM C1437-20, 2020) between 180 and 200 mm, as shown in Table 1. Constant consistency is essential in comparing the properties of different mortars. After mixing in accordance with ASTM C109/109M (2021), 50-mm cubic test specimens (4 per age) were molded and cured in a water lime-saturated solution until the testing ages (7, 28, and 120 days), with tests performed in a Shimadzu UH-F500kNI machine operating at 0.5 mm/min.

Table 1
Superplasticizer content and flow-table spreading of the mortars studied.

Mortar	Superplastisizer content (%)[a]	Flow-table spreading (mm)
M-REF	0.09	180
M-SBFA10	0.14	200
M-SBFA20	0.16	200
M-SBFA30	0.20	180

[a] Content in relation to binder mass.

Mortar durability under acid attack was determined based on mass variation, total absorption, absorption by capillarity, and compressive strength, before and after immersion in a 1.5% sulfuric acid solution for 92 days. The solution-to-mortar volume ratio was fixed at 4 and the variation in solution pH and specimen mass was monitored during the attack period. The pH was kept below 2.0 and two solution changes were needed (at 28 and 56 days of attack). At the beginning (after 28 days of limewater curing) and end of attack, four cubic test specimens (50 mm edge) were used in total water absorption tests (ASTM C642-21, 2021) and three cylindrical specimens (50 mm in diameter and 100 mm thick) for absorption by capillarity (ASTM C1585, 2020), lasting 28 days. Compressive strength tests were also carried out after acid attack, using five cubic specimens, with their upper and lower surfaces covered by a thin layer of high strength gypsum paste. Mortar results were subjected to statistical analysis (Analysis of Variance) to determine if significant differences ($p \leq 0.05$) could be observed among the mixes.

2.5. Evaluation of mix packing density

The packing density of dry mixes was obtained using Betonlab Pro 3 software, based on the Compressible Packing Model (CPM). This model is described in full by De Larrard (1999) and makes it possible to predict the actual packing density (φ) of a granular mix based on the particle size distribution and virtual packing density (γ) of each granular class of the different materials. A scalar parameter known as the compaction index (K) establishes the link between γ and φ. Within this framework, the compaction index K is closely linked to the protocol used for a given mix, and notably, as K tends to infinity, φ converges towards γ, as shown in Eq. (1).

$$K = \sum_{i=1}^{n} \frac{\frac{y_i}{\beta_i}}{\frac{1}{\varphi} - \frac{1}{\gamma^{(i)}}} \quad (1)$$

Considering n is the number of particle classes; y_i the volume fraction; β_i the virtual packing density of the ith class; and $\gamma^{(i)}$ the virtual packing density when i is the dominant class. The index K assumes a value of 4.5 when compaction occurs by simple pouring, 6.7 for water demand and 9.0 when the placing process is vibration followed by compression with 10 kPa of pressure.

In order to apply the CPM, the packing parameters of sand and fine materials must first be determined, both of which are described by De Larrard (1999). For sand, the vibration and compaction test ($K = 9$) was used, considering Eq. (2). The experimental packing densities of cement and binary cement-SBFA samples under wet conditions with 0.02 wt% superplasticizer were assessed via the water demand test ($K = 6.7$) described by De Larrard (1999), and calculated according to Eq. (3).

$$\varphi = \left(1 + \delta \frac{m_w}{m_b}\right)^{-1} \quad (2)$$

$$\varphi = m_s (V\delta)^{-1} \quad (3)$$

Considering δ is the sample density, m_w the mass of water, m_b the mass of the fine material (cement or cement-SBFA mix), m_s the mass of sand, and V the final volume of sand.

3. Results and discussion

3.1. Characterization of SBFA samples

SBFA was predominantly composed of SiO_2 (67.7%), as shown in Table 2. This silica content is very similar to that obtained for SCBA samples produced under controlled calcination (Cordeiro et al., 2009; Subedi et al., 2019). In addition to SiO_2, the main constituents of the ash were Al_2O_3 (12.1%), CaO (5.0%), K_2O (4.9%), Fe_2O_3 (3.7%), and SO_3 (2.3%). These concentrations are considerably lower than those reported by Bahurudeen et al. (2014) for a sugarcane fly ash, indicating low contamination. In this case, the presence of K_2O is due to fertilizers used in sugarcane production and/or nutrients from the soil, requiring careful mix-design of cementitious products with SBFA given the possibility of alkali-aggregate reactions in certain applications (Zhang et al., 2020). Loss on ignition (LOI) for SBFA (2.8%) was low and smaller than the value recorded in ashes collected by Mali and Nanthagopalan (2020) over an entire growing season. This demonstrates the excellent quality of the ash separated from the boiler flue gas in terms of contamination by carbonaceous materials. Under these circumstances, SBFA complied with ASTM C618-23e1 (2023), which stipulates LOI smaller than 10% for pozzolanic materials. It should be noted that this standard determines that the sum of SiO_2, Al_2O_3, and Fe_2O_3 should be at least 70%, which was also met by the SBFA studied.

Fig. 2 shows the X-ray diffraction pattern of SBFA, revealing the presence of quartz as the only crystalline phase and an amorphous halo between 15 and 30°, which is better visualized in the inset. Rietveld quantification indicated that the ash contained 44% quartz, suggesting an estimated amorphous silica content of around 24%, since the total SiO_2 content was 67.7% (Table 2). This amount of amorphous silica is similar to that observed for pozzolanic SCBA in different studies (Cordeiro et al., 2011; Mali and Nanthagopalan, 2021a). However, quartz content was lower than that recorded for bagasse ash (Moretti et al., 2018; Mali and Nanthagopalan, 2021a). This is an interesting characteristic of SBFA associated with the method used to collect the ash from the boiler exhaust stack. It is important to underscore that there is no crystalline phase in SBFA related to the 12.1% Al_2O_3, which further confirms the pozzolanic potential of this type of bagasse ash. It should further be noted that under the conditions adopted in the present study, grinding did not significantly alter the mineralogical composition of the bagasse fly ash, as previously observed in grinding of high purity crystalline silica (Palaniandy et al., 2007).

Fig. 3 shows the particle size distribution curves of the three ashes compared with that of cement. SBFA30 achieved a characteristic D_{50} of 30.3 μm (Table 3) after homogenization of the ashes collected at different times. This was performed in a ball mill for only 12 min and eliminated one of the problems of this type of ash, namely particle size variability (Cordeiro et al., 2016). In turn, SBFA20 and SBFA10 obtained D_{50} values of 19.9 and 9.9 μm, respectively, as defined by the grinding strategies adopted. SBFA20 displayed similar particle size distribution of class G cement. Based on a grinding study by Cordeiro et al. (2019) for a SCBA with 63.3% SiO_2, 8.1% Al_2O_3, 3.2% LOI, and D_{50} of 10 μm, SBFA10 could be produced by closed-circuit dry grinding in an industrial ball mill equipped with a classifier, and energy expenditure of around 40 kWh/t. This is about 50% lower than the energy consumed in the comminution of Portland cement, which includes crushing and grinding of raw materials and clinker grinding (Hosten and Fidan, 2012). The production of SBFA20, and evidently SBFA30, would provide

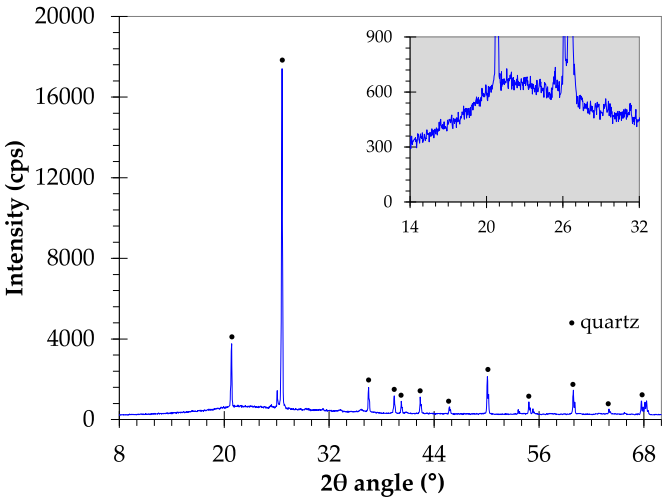

Fig. 2. X-ray diffraction pattern of SBFA.

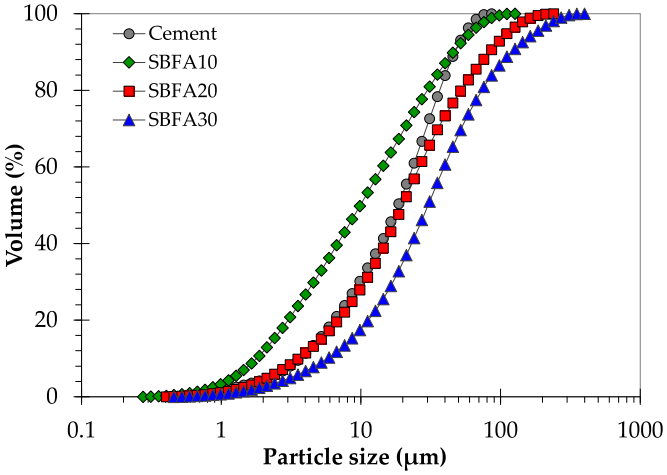

Fig. 3. Particle size distribution of SBFA10, SBFA20, SBFA30, and class G cement.

Table 2
Oxide composition and loss on ignition of SBFA and cement (%, in mass).

Oxide	SBFA	Cement
SiO_2	67.7	21.9
Al_2O_3	12.1	3.6
Fe_2O_3	3.7	4.5
CaO	5.0	64.3
K_2O	4.9	0.3
SO_3	2.3	2.7
P_2O_5	0.6	–
TiO_2	0.8	–
MnO	0.1	–
MgO	–	1.5
Na_2O	–	0.1
Loss on ignition	2.8	1.1

Table 3
Properties of SBFA10, SBFA20, and SBFA30.

Property	SBFA10	SBFA20	SBFA30
D_{50} (μm)	9.9	19.9	30.3
BET specific surface area (m^2/g)	16.2	13.9	17.1
Performance index (%)	133	118	113
Lime reactivity (MPa)	8.2	7.1	7.1
Modified Chapelle activity (mg/g)	530	485	465

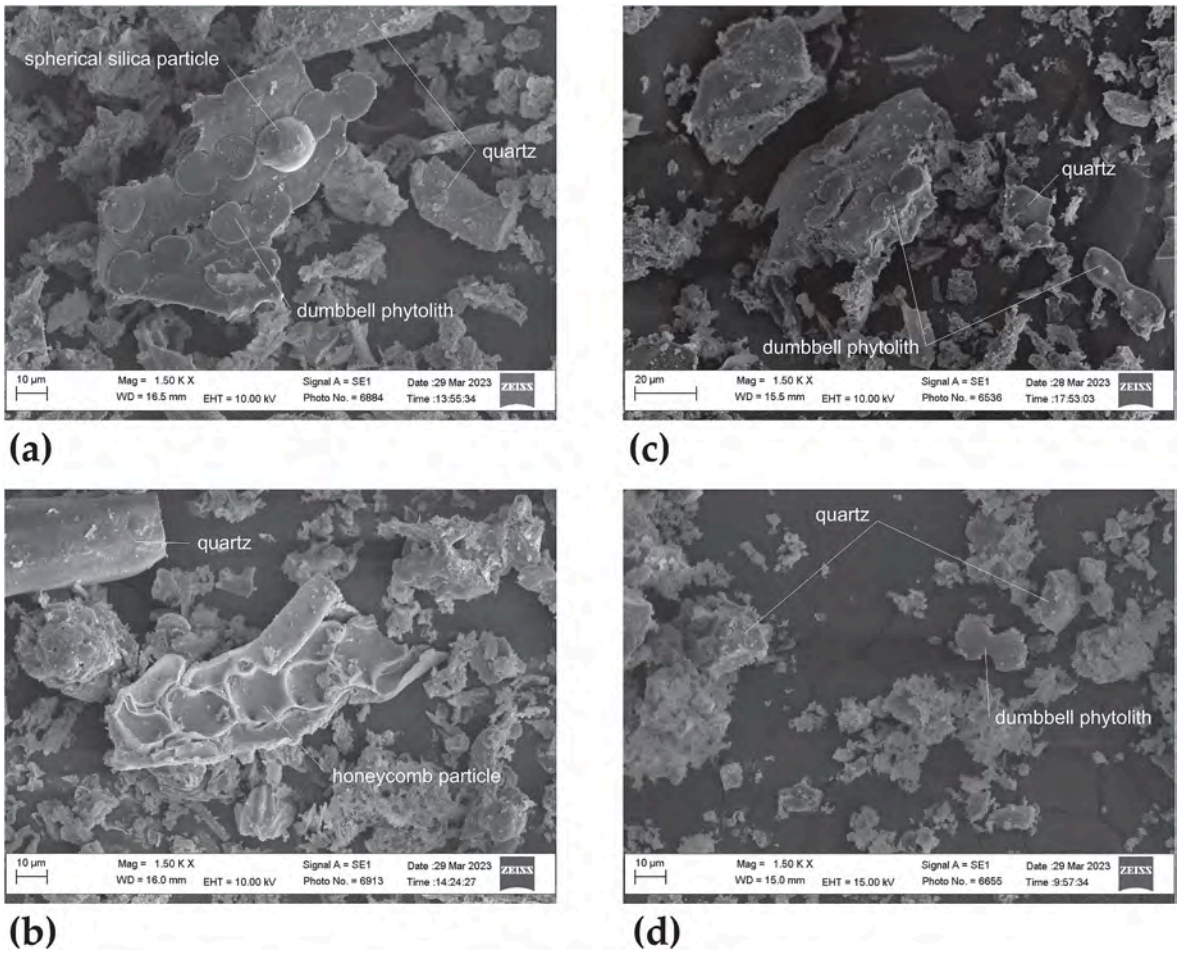

Fig. 4. SEM images of SBFA30 (a and b), SBFA20 (c), and SBFA10 (d) particles.

even greater energy savings in relation to clinker, which is relevant in producing cement with less environmental impact.

The different morphologies of the ash particles are shown in Fig. 4. SBFA30 (Fig. 4a) is composed of spherical particles typical of partially molten silica (Mali and Nanthagopalan, 2021a), siliceous bodies as a dumbbell-shaped phytolith chain cell structure (Roselló et al., 2015), and irregular quartz particles. Additionally, the honeycomb shape previously observed in sugarcane straw (Cordeiro et al., 2017), sugarcane bagasse (Batool et al., 2020), and elephant grass (Cordeiro and Sales, 2016) ashes, is also evident in SBFA30 (Fig. 4b). SBFA20 (Fig. 4c) exhibited a porous structure and dumbbell-shaped phytoliths even at a longer grinding time than that of SBFA30, and small quartz particles. Typical morphological structures were more difficult to discern in SBFA10 (Fig. 4d), as previously observed in sugarcane bagasse ash (Driemeier et al., 2011) associated to grinding time, but dumbbell-shaped phytoliths and quartz were observed.

The gas adsorption-desorption isotherms of the bagasse fly ashes are shown in Fig. 5 and reveal that all the ashes can be classified as H3 Type II according to IUPAC guidelines (Thommes et al., 2015). This means that these ashes contain a network of meso and macropores, evident in the morphologies shown in Fig. 4. SBFA30 absorbed a slightly higher volume of gas than the other ashes, demonstrating that its particles are more porous, corroborating the SEM analyses (Fig. 4). In fact, the BET specific surface area of SBFA30 (17.1 m^2/g) was greater than that of SBFA20 (13.9 m^2/g), as shown in Table 3. This phenomenon of a decrease in specific surface area with an increase in grinding time seems contradictory, but was previously reported in research on grinding rice husk ash (Cordeiro et al., 2011; Van et al., 2013; Vieira et al., 2020). The

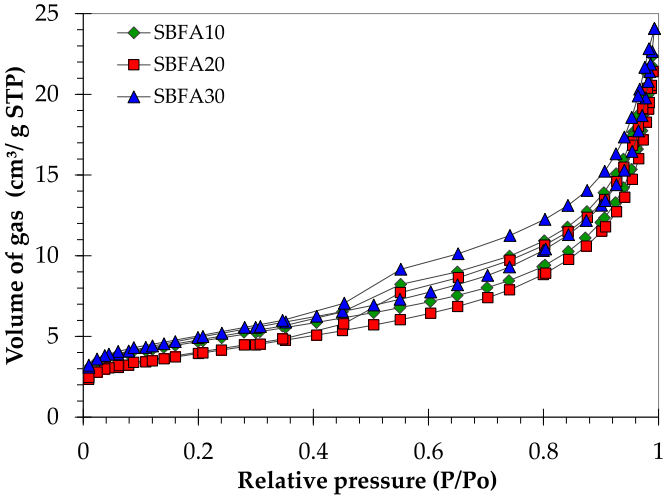

Fig. 5. Adsorption-desorption isotherms of SBFA10, SBFA20, and SBFA30.

reduction in specific surface area associated with the decline in D_{50} from 30 to 20 μm is related to the collapse of the porous structure under mild grinding conditions, such as those used to produce SBFA20. With longer grinding time, the specific surface area increased as expected, since SBFA10 reached a BET value of 16.2 m^2/g. The specific surface area values of the SBFA samples are consistent with those obtained for sugarcane bagasse ash produced under laboratory conditions (Figueiredo

and Pavía, 2020).

The results of performance index tests (Table 3) demonstrated that the three ashes obtained higher values than the minimum 90%, complying with ABNT NBR 12653 (2014) requirements. SBFA10 obtained the highest performance index (133%) among the ashes assessed, followed by SBFA20 (118%) and SBFA30 (113%). In this case, even the ash submitted only to homogenization showed high pozzolanic activity considering its influence on the mechanical performance of the mortar produced. The smaller particle size improved the performance index, which corroborates the behavior observed for sugarcane bagasse ash (Cordeiro and Kurtis, 2017; Mali and Nanthagopalan, 2021b). The minor variation in specific surface area seems to have less effect on the pozzolanic activity of the ashes than the change in particle size, as previously reported for rice husk ash (Cordeiro et al., 2011). The lime reactivity tests indicated in Table 3 corroborated the performance index results. In this case, the mortars containing SBFA30 and SBFA20 obtained the same compressive strength value (7.1 MPa) after 7 days of curing. However, SBFA10 entailed a significant increase (approximately 15%) in mortar compressive strength in relation to the mixes with the other ashes. This behavior confirmed the greater activity of the finer ash, whose lime reactivity was similar to that of a pozzolanic fly ash evaluated using the same methodology (Kasaniya et al., 2019).

The modified Chapelle test provided a more accurate view of the pozzolanic behavior of bagasse fly ashes in relation to different particle sizes and BET specific surface areas. This methodology, based on hydroxide consumption under calcium supersaturation, showed a considerable increase in activity due to the decline in particle size, as shown in the results presented in Table 3. SBFA10 displayed Chapelle activity of 530 mg/g, while the remaining ashes obtained reactivity of 485 (SBFA20) and 465 mg/g (SBFA30). The rise in pozzolanic activity with reduced particle size may be associated with the increased exposure of amorphous silica promoted by grinding. Cordeiro and Kurtis (2017) observed a significant increase in solubility in an alkaline environment of the silica in bagasse ash at smaller particle sizes. The Chapelle pozzolanic activity values obtained by the bagasse fly ashes were significantly higher than those recorded for different SCBA samples (Cordeiro et al., 2018a; Mali and Nanthagopalan, 2021a). Fig. 6 shows the correlations between performance index and lime reactivity with Chapelle activity for the three ashes studied. Both mechanical tests showed a good linear relationship (coefficients of determination greater than 0.9) with Chapelle activity, indicating that the performance gains in the cement or lime-based mortars containing SBFA were largely due to the increased pozzolanic activity of the ashes provided by the reduced particle size of the bagasse fly ash. In this case, the significance of particle reduction is evident, representing a tangible advantage of this fly ash over traditional sugarcane bagasse ashes in terms of grinding.

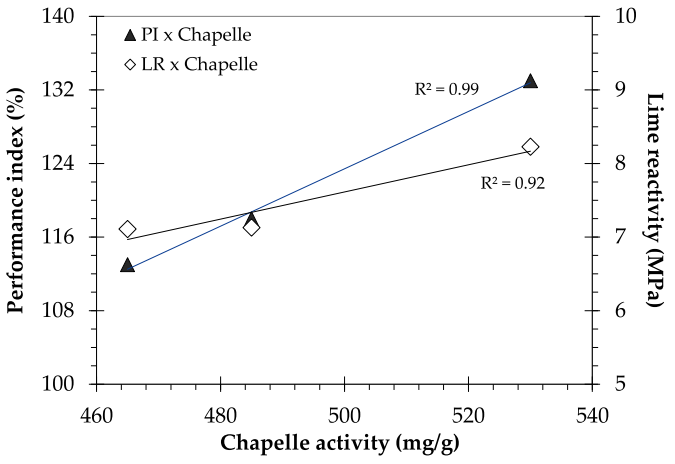

Fig. 6. Linear correlations between performance index (PI) and Chapelle activity and between lime reactivity (LR) and Chapelle activity.

3.2. Cement-based paste hydration kinetics

Fig. 7 shows the isothermal calorimetry results of the pastes calculated based on their binder mass. By analyzing the heat flow curves after the first exothermic peak, the pastes with SBFA showed a slightly shorter induction period than that of P-REF, evident in the inset of Fig. 7a. This effect is associated with the heterogeneous nucleation promoted by including SBFA particles with a large specific surface area and increasing the water-to-cement ratio, which improves cement hydration in the initial minutes (Ali et al., 2022). There was also a 5% decline in maximum heat flow after the induction period in the pastes with SBFA when compared to P-REF, demonstrating the better hydration provided by 20% cement replacement with ash. This behavior was reported in studies with cement-based pastes containing SCBA (Barbosa and Cordeiro, 2021; De Siqueira and Cordeiro, 2022). The peak related to sulfate depletion occurred earlier in ash pastes than the reference. In this case, the high Al_2O_3 and SO_3 content in bagasse fly ashes contributed to this behavior (Maldonado-García et al., 2018).

The curves of cumulative released heat per gram of binder (Fig. 7b) demonstrated slightly less released heat for P-SBFA10, P-SBFA20, and P-SBFA30 than P-REF. This approximate 6% decline (about 250 J/g for P-REF and 235 J/g for SBFA mixes) was considerably lower than the cement replacement content used in the pastes and demonstrated the positive effect of the ashes on cement hydration. This behavior is even more evident in the inset of Fig. 7b, which shows the heat release curves

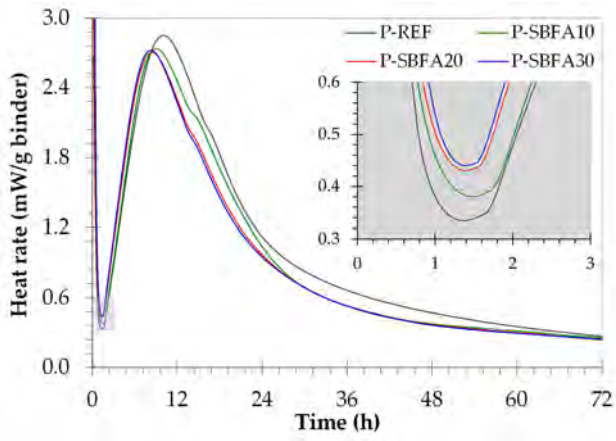

(a)

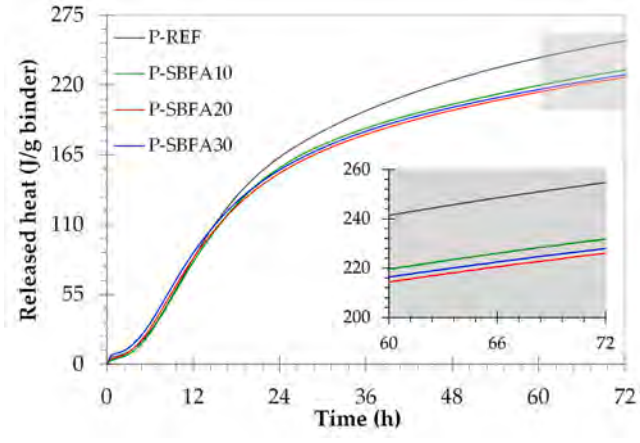

(b)

Fig. 7. Specific heat rate (a) and released heat (b) curves calculated based on binder mass for all the pastes. Insets show the induction period (a) and final 12 h of released heat (b).

calculated as a function of binder mass in each paste on the last day of testing. The greater heat released by SBFA pastes and small difference in heat between them after three days of hydration was also evident. The minimal difference between the BET specific surface areas of the three SBFA samples studied explained the similar behavior of the pastes. It is important to note that P-SBFA10 showed greater 72-h released heat among the ash-containing pastes, corroborating the pozzolanic activity results shown in Table 3.

3.3. Evolution of mortar compressive strength over time

The average compressive strength values of the mortars at 7, 28, and 120 days are shown in Fig. 8. At 7 days, M-REF, M-SBFA10, and M-SBFA20 exhibited compressive strength of about 26 MPa and no significant differences between means at 5% probability from analysis of variance. At this age, the mean strength of M-SBFA30 was about 20% lower than that recorded for the remaining mortars. The difference in reactivity between the ashes, albeit small, promoted a significant difference between the mix containing coarser-grained ash in relation to the remaining mixes.

After 28 days of curing, there were statistically significant differences in compressive strength. The superior performance of M-SBFA10, which exhibited a strength of 37 MPa, supported the results of pozzolanic activity and isothermal calorimetry. It is worth noting that P-SBFA10 already showed a higher heat release after 3 days of hydration. The slow pozzolanic reactions observed for sugarcane bagasse ash (Embong et al., 2016; Cordeiro et al., 2018a) were also observed for SBFA. This effect was also noted by Bahurudeen et al. (2015), who studied concretes with 10 and 20% cement replacement by SCBA. At 28 days, the strength of the reference mortar was 34.8 MPa, while the mean value for M-SBFA20 was 33.1 MPa. M-SBFA30 remained the weakest mix at 28 days, with a 15% decline in relation to M-REF and 20% when compared with M-SBFA10.

The pozzolanic effect of SBFA10 and SBFA20 was confirmed in long-term compressive strength testing at 120 days of curing, as previously observed in SCBA samples with moderate pozzolanic activity (Cordeiro et al., 2018b; Maldonado-García et al., 2018). There was no significant difference between the average strength values of M-SBFA10 and SBFA20 and both mortars exhibited superior strength to that of M-REF (8% increase). M-SBFA30 also showed lower strength at this final testing age, although the significant difference in relation to M-REF declined to 12%. This indicates that for a 20% replacement content, the dilution effect overcame the moderate pozzolanic activity of the material, which was more evident in long-term testing. In general, the compressive strength results suggested that an SBFA with a D_{50} similar to that of cement can be used for long-term strength gains. This is an important characteristic and confers greater added value to ash, since ultrafine grinding is not necessary in this case. More in-depth grinding studies can confirm this behavior and enable a correlation between the energy consumed in grinding and short and long-term strength gains in cementitious systems.

3.4. Durability of mortars under sulfuric acid attack

Exposing the different mortars to 1.5% sulfuric acid solution resulted in visible degradation and associated mass loss that gradually increased over time, as shown in Fig. 9. In general, all the mixes containing SBFA showed less mass loss than that of M-REF. Until around 35 days of exposure, there were no statistically significant differences between the mortars containing the three ashes, with cumulative mass loss of approximately 5% compared to 15% for M-REF. After this age, M-SBFA30 exhibited the greatest mass loss among the ash-based mixes, which persisted until the end of the exposure period. The attack was interrupted when M-REF reached approximately 44% mass loss, which was higher than those recorded for M-SBFA30 (35%), M-SBFA20 (27%), and M-SBFA10 (25%).

At first glance, the lower mass loss of the mortars containing SBFA may suggest less degradation under acid attack, as previously described by Senhadji et al. (2014) and Arif et al. (2016) in studies with silica fume and SCBA, respectively. However, analysis of the middle section of the test specimens after attack showed a completely different degradation mechanism in SBFA mortars when compared with M-REF. The test specimens of mixes containing ash retained a degraded layer basically consisting of gypsum adhered to the preserved core, according to X-ray diffraction analysis (data not shown). The average thickness values of the degraded layers shown in Fig. 10 were 3.6, 5.6, and 4.0 mm in M-SBFA30, M-SBFA20, and M-SBFA10, respectively. In turn, M-REF showed no considerable adhered degraded layer (only 0.6 mm thick), justifying its greater mass loss over 92 days of acid attack (Fig. 9). This interesting behavior of the adhered degraded layer was also observed by De Siqueira and Cordeiro (2022) in a study on resistance to sulfuric acid attack in mixes of cements, SCBA, and limestone.

The presence of a degraded layer adhered to the test specimens considerably increased the total water absorption and water absorption by capillarity in the **Supplementary Data** with a detailed discussion. The formation of a degraded layer in the SBFA mixes significantly reduced the compressive strength of the mortars (Fig. 11). The degraded area covers a considerable portion of the cross-sectional area of the test specimens used to calculate compressive strength (specimens with

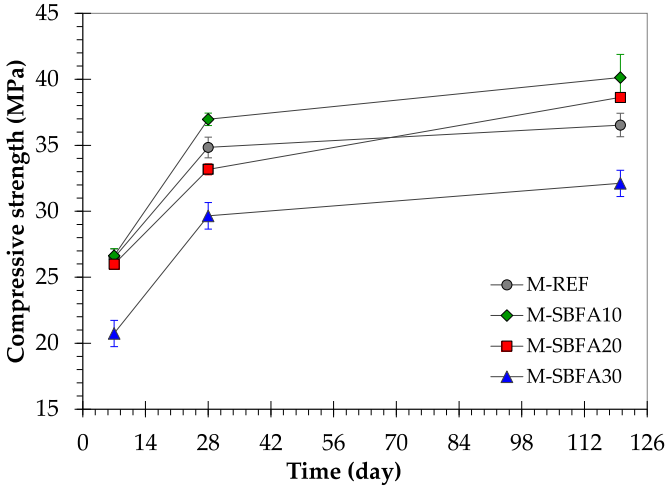

Fig. 8. Compressive strength of mortars at 7, 28, and 120 days of curing.

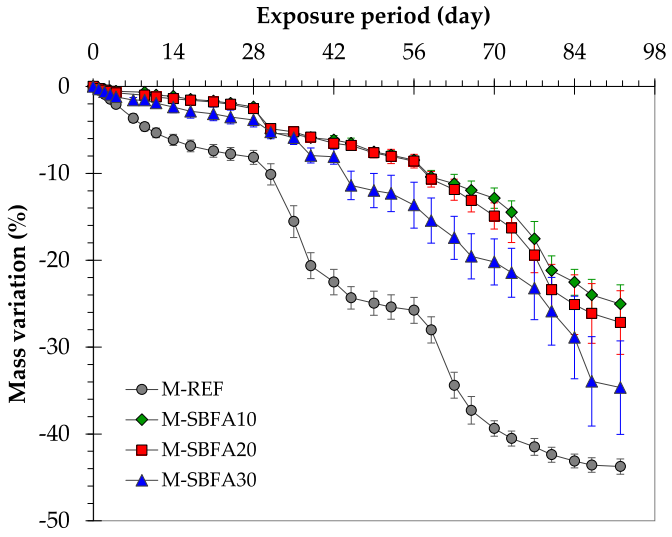

Fig. 9. Mass variations of mortars during sulfuric acid attack.

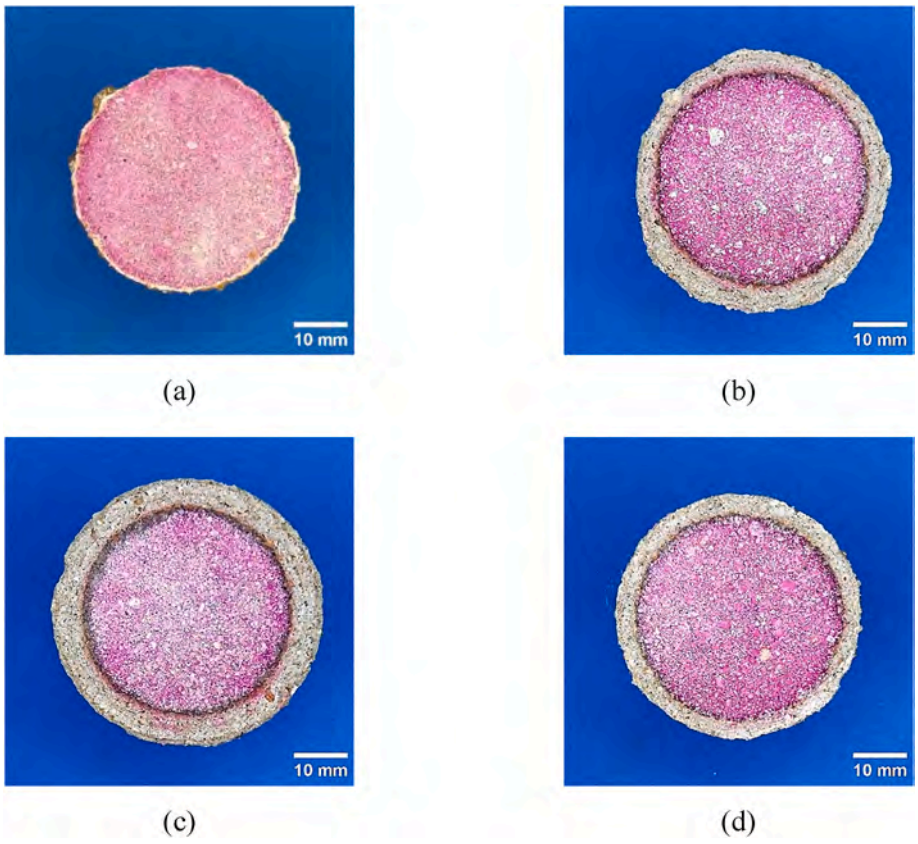

Fig. 10. Middle-section surface of the test specimens after 92 days of acid attack with phenolphthalein: M-REF (a), M-SBFA10 (b), M-SBFA20 (c), and M-SBFA30 (d).

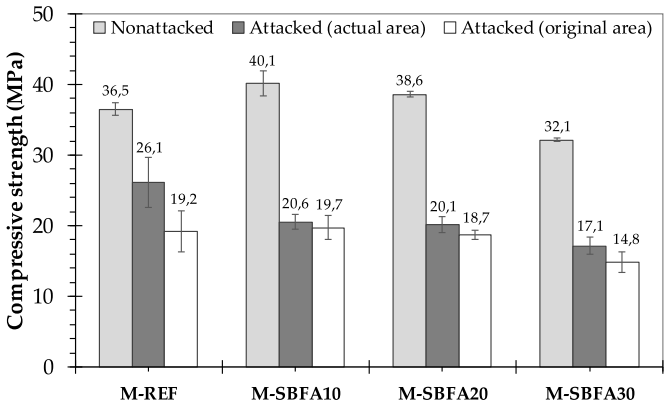

Fig. 11. Compressive strength at 120 days in nonattacked and attacked mortars (calculated considering actual and original areas).

actual area, as indicated in Fig. 11 legend). The reduced strength of the acid-attacked M-REF compared with the same mortar submitted to limewater curing indicated that degradation goes beyond the degraded layer and that the apparently intact core also sustained considerable damage. However, the more pronounced compressive strength decrease observed for M-SBFA30, M-SBFA20, and M-SBFA10 demonstrated that the degradation mechanism with the formation of a thick degraded layer significantly compromised mortar mechanical behavior. Praveenkumar and Sankarasubramanian (2021) observed an opposite behavior in concretes with up to 10% of SCBA, noting an increase in compressive strength attributed to the refinement of the porous structure.

Comparison of compressive strength values considering the original area of the specimens (measured before acid attack - about 25 cm^2) is also shown in Fig. 11, with no significant differences for M-REF, M-SBFA10, and M-SBFA20 after acid attack. In practical terms, that is, under structural service conditions, these three mixes would produce structures (e.g., sewage ducts) with the same bearing capacity. The considerable aggressiveness of the sulfuric acid attack with pH remaining below 2 explains this behavior.

3.5. Considerations on SBFA pozzolanic activity and packing density

Predicting the packing density of different dry mixes allowed some inferences regarding the strictly pozzolanic role of the ash and the contribution of physical effects resulting from particle size changes.

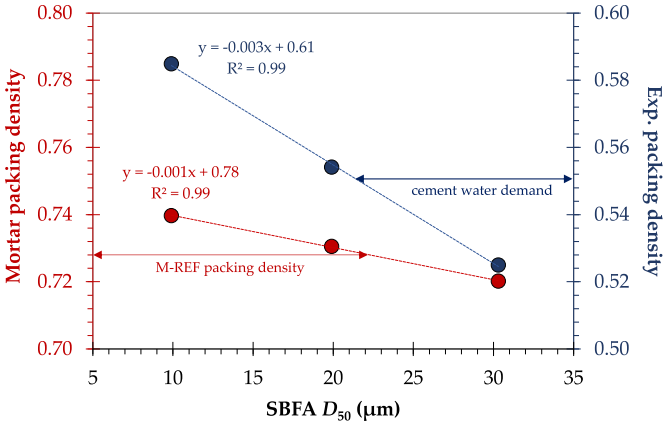

Fig. 12. Relationship between predicted mortar packing density (red symbols) and the experimental packing density of cement-SBFA (by water demand tests - blue symbols) and D_{50} of SBFA samples. (For interpretation of the references to colour in this figure legend, the reader is referred to the Web version of this article.)

Fig. 12 shows the good linear correlation (R^2 = 0.99) between the packing density of each mortar and the D_{50} value of the SBFA used in the respective mix. There was a clear increase in packing density when a finer ash is used in the mortar. The predominant role of ash particle size distribution in packing density was also evident in Fig. 12, since the packing density of the reference mortar was similar to that of the ash-containing mortar with the closest particle size to that of the cement, namely SBFA-20 (as shown in Fig. 3). This behavior corroborated the good correlation between the pozzolanicity results obtained in mechanical tests and activity resulting from the chemical action with calcium hydroxide (Fig. 6).

Finally, in accordance with Fig. 12, the effect of ash particle size on the water demand of cement-SBFA mixes was more significant than its influence on mortar packing density. This was due to the presence of sand occupying around 58% of mortar volume (or 77% of the volume of solids). These results corroborated those observed for SCBA samples with different particle size distributions (Cordeiro et al., 2016).

4. Conclusions

The following conclusions were drawn from the study on producing finely ground bagasse fly ash and its application in pastes and mortars. The chemical composition of the bagasse fly ash was suitable for use as a supplementary cementitious material, largely because of the presence of 24% amorphous silica and low loss on ignition (2.8%). Moreover, the ashes showed increased pozzolanic activity with a decline in particle size, resulting in accelerated hydration in the initial hours and greater long-term compressive strength of the mortars. A good correlation was observed between packing density and ash particle size, with finer ash resulting in higher mortar packing density. Thus, finer ash exhibited the best mechanical performance, although adequate ash can be produced with D_{50} of 20 μm. In terms of durability, the acid-attacked M-REF specimens experienced greater mass loss during sulfuric acid attack. However, given the different degradation mechanism of the attacked mortars containing SBFA samples, water absorption increased and compressive strength declined when compared with their nonattacked counterparts and the attacked reference specimens.

In summary, while the use of ultrafine bagasse fly ash in cementitious materials offers several advantages, such as enhanced mechanical performance, accelerated hydration, and environmental benefits, there are also limitations related to durability and mechanical performance with coarser particles. Overall, proper consideration of these factors is necessary for effective large-scale use of sugarcane bagasse fly ash in cementitious applications. Further research should focus on (i) understanding the long-term performance of cementitious materials containing bagasse fly ash; (ii) performing life-cycle assessments to evaluate the environmental impact of using bagasse fly ash as a supplementary cementitious material compared to conventional materials; (iii) investigating the economic feasibility of incorporating bagasse fly ash into cementitious materials, including cost-benefit analyses and assessing the potential for commercial-scale production. By addressing these research directions, further advances can be made in harnessing the potential of bagasse fly ash as a sustainable and effective supplementary cementitious material, contributing to the development of eco-friendly construction practices.

CRediT authorship contribution statement

Ketlynn Passos Alvarenga: Writing – original draft, Methodology, Investigation, Conceptualization. **Guilherme Chagas Cordeiro:** Writing – review & editing, Writing – original draft, Visualization, Supervision, Methodology, Conceptualization.

Declaration of competing interest

The authors declare that they have no known competing financial interests or personal relationships that could have appeared to influence the work reported in this paper.

Data availability

Data will be made available on request.

Acknowledgments

This study was financed in part by the Coordenação de Aperfeiçoamento de Pessoal de Nível Superior – Brasil (CAPES) - Finance Code 001. The authors would like to thank the Brazilian Conselho Nacional de Desenvolvimento Científico e Tecnológico (CNPq) and Fundação Carlos Chagas Filho de Amparo à Pesquisa do Estado do Rio de Janeiro (FAPERJ) for the additional funding provided.

Appendix A. Supplementary data

Supplementary data to this article can be found online at https://doi.org/10.1016/j.clet.2024.100751.

References

ABNT NBR 15895, 2010. Pozzolanic Materials - Determination of Calcium Hydroxide Fixed – Modified Chapelle's Method (in Portuguese).
ABNT NBR NM 18, 2012. Portland Cement - Chemical Analysis - Determination of Loss on Ignition (in Portuguese).
ABNT NBR 12653, 2014. Pozzolanic Materials - Requirements (in Portuguese).
ABNT NBR 5752, 2014. Pozzolanic Materials - Determination of the Performance Index with Portland Cement at 28 Days (in Portuguese).
ABNT NBR 7214, 2015. Standard Sand for Cement Tests - Specification (in Portuguese).
ABNT NBR 16605, 2017. Portland Cement and Other Powdered Material - Determination of the Specific Gravity (in Portuguese).
ABNT NBR 16697, 2018. Portland Cement - Requirements (in Portuguese).
ABNT NBR 9831, 2020. Oil Well Portland Cements - Requirements and Test Methods (in Portuguese).
Ahmad, W., Ahmad, A., Ostrowski, K.A., Aslam, F., Joyklad, P., Zajdel, P., 2021. Sustainable approach of using sugarcane bagasse ash in cement-based composites: a systematic review. Case Stud. Constr. Mater. 15, e00698 https://doi.org/10.1016/j.cscm.2021.e00698.
Ali, S.E., Azam, R., Riaz, M.R., Zawam, M., 2022. Effect of fineness of ash on pozzolanic properties and acid resistance of sugarcane bagasse ash replaced cement mortars. Front. Struct. Civ. Eng. 16, 1287–1300. https://doi.org/10.1007/s11709-022-0872-7.
Almeida, R.P.A., Cordeiro, G.C., 2023. Sustainable approach to simultaneously improve the pozzolanic activity of sugarcane bagasse ash and the vinasse fertilization potential. Clean. Eng. Technol. 13, 100617 https://doi.org/10.1016/j.clet.2023.100617.
Andreão, P.V., Suleiman, A.R., Cordeiro, G.C., Nehdi, M.L., 2020. Beneficiation of sugarcane bagasse ash: pozzolanic activity and leaching behavior. Waste Biomass Valori 11, 4393–4402. https://doi.org/10.1007/s12649-019-00721-x.
Arif, E., Clark, M.W., Lake, N., 2016. Sugar cane bagasse ash from a high efficiency co-generation boiler: applications in cement and mortar production. Construct. Build. Mater. 128, 287–297. https://doi.org/10.1016/j.conbuildmat.2016.10.091.
ASTM 1585, 2020. Standard Test Method for Measurement of Rate of Absorption of Water by Hydraulic Cement Concretes.
ASTM C1437-20, 2020. Standard Test Method for Flow of Hydraulic Cement Mortar.
ASTM C109/109M-21, 2021. Standard Test Method for Compressive Strength of Hydraulic Cement Mortars (Using 2-in. Or [50-mm] Cube Specimens).
ASTM C642-21, 2021. Standard Test Method for Density, Absorption, and Voids in Hardened Concrete.
ASTM C618-23e1, 2023. Standard Specification for Coal Ash and Raw or Calcined Natural Pozzolan for Use in Concrete.
Bahurudeen, A., Kanraj, D., Dev, V.G., Santhanam, M., 2015. Performance evaluation of sugarcane bagasse ash blended cement in concrete. Cem. Concr. Compos. 59, 77–88. https://doi.org/10.1016/j.cemconcomp.2015.03.004.
Bahurudeen, A., Marckson, A.V., Kishore, A., Santhanam, M., 2014. Development of sugarcane bagasse ash based Portland pozzolana cement and evaluation of compatibility with superplasticizers. Construct. Build. Mater. 68, 465–475. https://doi.org/10.1016/j.conbuildmat.2014.07.013.
Barbosa, F.L., Cordeiro, G.C., 2021. Partial cement replacement by different sugar cane bagasse ashes: hydration-related properties, compressive strength and autogenous shrinkage. Construct. Build. Mater. 272, 121625 https://doi.org/10.1016/j.conbuildmat.2020.121625.
Batool, F., Masood, A., Ali, M., 2020. Characterization of sugarcane bagasse ash as pozzolan and influence on concrete properties. Arabian J. Sci. Eng. 45, 3891–3900. https://doi.org/10.1007/s13369-019-04301-y.

Cordeiro, G.C., Andreão, P.V., Tavares, L.M., 2019. Pozzolanic properties of ultrafine sugar cane bagasse ash produced by controlled burning. Heliyon 5 (10), e02566. https://doi.org/10.1016/j.heliyon.2019.e02566.

Cordeiro, G.C., Kurtis, K.E., 2017. Effect of mechanical processing on sugar cane bagasse ash pozzolanicity. Cement Concr. Res. 97, 41–49. https://doi.org/10.1016/j.cemconres.2017.03.008.

Cordeiro, G.C., Barroso, T.R., Toledo Filho, R.D., 2018a. Enhancement the properties of sugar cane bagasse ash with high carbon content by a controlled re-calcination process. KSCE J. Civ. Eng. 22, 1250–1257. https://doi.org/10.1007/s12205-017-0881-6.

Cordeiro, G.C., Paiva, O.A., Toledo Filho, R.D., Fairbairn, E.M.R., Tavares, L.M., 2018b. Long term compressive behavior of concretes with sugarcane bagasse ash as a supplementary cementitious material. J. Test. Eval. 46, 564–573. https://doi.org/10.1520/JTE20160316.

Cordeiro, G.C., Sales, C.P., 2016. Influence of calcining temperature on the pozzolanic characteristics of elephant grass ash. Cem. Concr. Compos. 73, 98–104. https://doi.org/10.1016/j.cemconcomp.2016.07.008.

Cordeiro, G.C., Tavares, L.M., Toledo Filho, R.D., 2016. Improved pozzolanic activity of sugar cane bagasse ash by selective grinding and classification. Cement Concr. Res. 89, 269–275. https://doi.org/10.1016/j.cemconres.2016.08.020.

Cordeiro, G.C., Toledo Filho, R.D., Fairbairn, E.M.R., 2009. Effect of calcination temperature on the pozzolanic activity of sugar cane bagasse ash. Construct. Build. Mater. 23 (10), 3301–3303. https://doi.org/10.1016/j.conbuildmat.2009.02.013.

Cordeiro, G.C., Toledo Filho, R.D., Tavares, L.M., Fairbairn, E.M.R., Hempel, S., 2011. Influence of particle size and specific surface area on the pozzolanic activity of residual rice husk ash. Cement Concr. Compos. 33 (5), 529–534. https://doi.org/10.1016/j.cemconcomp.2011.02.005.

Cordeiro, G.C., Vieira, A.P., Lopes, E.S., 2017. Study on the pozzolanic activity of sugar cane straw ash produced using different pretreatments. Quím. Nova 40 (3), 264–269. https://doi.org/10.21577/0100-4042.20170002.

de Almeida, S.G.C., Fogarin, H.M., Costa, M.A.M., Dussán, K.J., 2023. Study of sugarcane bagasse/straw combustion and its atmospheric emissions using a pilot-burner. Environ. Sci. Pollut. 31 (12), 17706–17717. https://doi.org/10.1007/s11356-023-28171-y.

de Larrard, F., 1999. Concrete Mixture Proportioning: a Scientific Approach, 1 ed. E&FN Spon, London, p. 421.

de Siqueira, A.A., Cordeiro, G.C., 2022. Properties of binary and ternary mixes of cement, sugarcane bagasse ash and limestone. Construct. Build. Mater. 317, 126150 https://doi.org/10.1016/j.conbuildmat.2021.126150.

Driemeier, C., Oliveira, M.M., Mendes, F.M., Gómez, E.O., 2011. Characterization of sugarcane bagasse powders. Powder Technol. 214, 111–116. https://doi.org/10.1016/j.powtec.2011.07.043.

Embong, R., Shafiq, N., Kusbiantoro, A., Nuruddin, M.F., 2016. Effectiveness of low-concentration acid and solar drying as pre-treatment features for producing pozzolanic sugarcane bagasse ash. J. Clean. Prod. 112, 953–962. https://doi.org/10.1016/j.jclepro.2015.09.066.

Figueiredo, R.L., Pavía, S., 2020. A study of the parameters that determine the reactivity of sugarcane bagasse ashes (SCBA) for use as a binder in Construction. SN Appl. Sci. 2 (9) https://doi.org/10.1007/s42452-020-03224-w.

Hosten, C., Fidan, B., 2012. An industrial comparative study of cement clinker grinding systems regarding the specific energy consumption and cement properties. Powder Technol. 221, 183–188. https://doi.org/10.1016/j.powtec.2011.12.065.

Kasaniya, M., Thomas, M.D.A., Moffatt, E.G., 2019. Development of a rapid and reliable pozzolanic reactivity test method. ACI Mater. J. 116, 145–154. https://doi.org/10.14359/51716718.

Liu, H., Kuo, C., 1996. Quantitative multiphase determination using the Rietveld method with high accuracy. Mater. Lett. 26, 171–175. https://doi.org/10.1016/0167-577X(95)00221-9.

Maldonado-García, M.A., Hernández-Toledo, U.I., Montes-García, P., Valdez-Tamez, P.L., 2018. The influence of untreated sugarcane bagasse ash on the microstructural and mechanical properties of mortars. Mater. Construcción 68 (329), 148. https://doi.org/10.3989/mc.2018.13716.

Mali, A.K., Nanthagopalan, P., 2020. A systematic assessment for the determination of sugarcane bagasse ash variation potential throughout the harvesting season. Mater. Today: Proc. 32, 888–895. https://doi.org/10.1016/j.matpr.2020.04.511.

Mali, A.K., Nanthagopalan, P., 2021a. Development of a framework for the selection of best sugarcane bagasse ash from different sources for use in the cement-based system: a rapid and reliable path. Construct. Build. Mater. 293, 123386 https://doi.org/10.1016/j.conbuildmat.2021.123386.

Mali, A.K., Nanthagopalan, P., 2021b. Comminution: a supplementation for pozzolanic adaptation of sugarcane bagasse ash. J. Mater. Civ. Eng. 33 (12), 04021343 https://doi.org/10.1061/(asce)mt.1943-5533.0003985.

Minnu, S., Bahurudeen, A., Athira, G., 2021. Comparison of sugarcane bagasse ash with fly ash and slag: an approach towards industrial acceptance of sugar industry waste in cleaner production of cement. J. Clean. Prod. 285, 124836 https://doi.org/10.1016/j.jclepro.2020.124836.

Mohan, B., Ma, S., Kumar, S., Yang, Y., Ren, P., 2023. Tactile sensors: hydroxyl decorated silver metal-organic frameworks for detecting $Cr_2O_7^{2-}$, MnO_4^-, humic acid, and Fe^{3+} ions. ACS Appl. Mater. Interfaces 15, 17317–17323. https://doi.org/10.1021/acsami.2c22871.

Moretti, J.P., Sales, A., Quarcioni, V.A., Silva, D.C.B., Oliveira, M.C.B., Pinto, N.S., Ramos, L.W.S.L., 2018. Pore size distribution of mortars produced with agroindustrial waste. J. Clean. Prod. 187, 473–484. https://doi.org/10.1016/j.jclepro.2018.03.219.

Nassar, R., Singh, N., Varsha, S., Sai, A.R., Sufyan-Ud-Din, M., 2022. Strength, electrical resistivity and sulfate attack resistance of blended mortars produced with agriculture waste ashes. Case Stud. Constr. Mater. 16, e00944 https://doi.org/10.1016/j.cscm.2022.e00944.

Palaniandy, S., Azizli, K.A.M., Hussin, H., Hashim, S.F.S., 2007. Study on mechanochemical effect of silica for short grinding period. Int. J. Miner. Process. 82, 195–202. https://doi.org/10.1016/j.minpro.2006.10.008.

Praveenkumar, S., Sankarasubramanian, G., 2021. Synergic effect of sugarcane bagasse ash based cement on high performance concrete properties. Silicon 13, 2357–2367. https://doi.org/10.1007/s12633-020-00832-4.

Roselló, J., Soriano, L., Santamarina, M.P., Akasaki, J.L., Melges, J.L.P., Payá, J., 2015. Microscopy characterization of silica-rich agrowastes to be used in cement binders: bamboo and sugarcane leaves. Microsc. Microanal. 21, 1314–1326. https://doi.org/10.1017/s1431927615015019.

Sales, A., Lima, S.A., 2010. Use of Brazilian sugarcane bagasse ash in concrete as sand replacement. Waste Manag. 30, 1114–1122. https://doi.org/10.1016/j.wasman.2010.01.026.

Senhadji, Y., Escadeillas, G., Mouli, M., Khelafi, H.Benosman, 2014. Influence of natural pozzolan, silica fume and limestone fine on strength, acid resistance and microstructure of mortar. Powder Technol. 254, 314–323. https://doi.org/10.1016/j.powtec.2014.01.046.

Subedi, S., Arce, G., Hassan, M., Kumar, N., Barbato, M., Gutierrez-Wing, M.T., 2019. Influence of production methodology on the pozzolanic activity of sugarcane bagasse ash. MATEC Web Conf. 271, 07003 https://doi.org/10.1051/matecconf/201927107003.

Thommes, M., Kaneko, K., Neimark, A.V., Olivier, J.P., Rodriguez-Reinoso, F., Rouquerol, J., Sing, K.S.W., 2015. Physisorption of gases, with special reference to the evaluation of surface area and pore size distribution (IUPAC Technical Report). Pure Appl. Chem. 87, 1051–1069. https://doi.org/10.1515/pac-2014-1117.

Van, V., Rößler, C., Bui, D., Ludwig, H., 2013. Mesoporous structure and pozzolanic reactivity of rice husk ash in cementitious system. Construct. Build. Mater. 43, 208–216. https://doi.org/10.1016/j.conbuildmat.2013.02.004.

Vieira, A.P., Toledo Filho, R.D., Tavares, L.M., Cordeiro, G.C., 2020. Effect of particle size, porous structure and content of rice husk ash on the hydration process and compressive strength evolution of concrete. Construct. Build. Mater. 236, 117553 https://doi.org/10.1016/j.conbuildmat.2019.117553.

Zhang, P., Liao, W., Kumar, A., Zhang, Q., Ma, H., 2020. Characterization of sugarcane bagasse ash as a potential supplementary cementitious material: comparison with coal combustion fly ash. J. Clean. Prod. 277, 123834 https://doi.org/10.1016/j.jclepro.2020.123834.